Monthly Notices
of the
ROYAL ASTRONOMICAL SOCIETY

MNRAS **435,** 1037–1046 (2013) doi:10.1093/mnras/stt1293
Advance Access publication 2013 August 30

First results of the SONS survey: submillimetre detections of debris discs

O. Panić,[1]⋆ W. S. Holland,[2,3] M. C. Wyatt,[1] G. M. Kennedy,[1] B. C. Matthews,[4,5] J. F. Lestrade,[6] B. Sibthorpe,[7] J. S. Greaves,[8] J. P. Marshall,[9] N. M. Phillips[10] and J. Tottle[11]

[1]*Institute of Astronomy, Madingley Road, Cambridge CB3 0HA, UK*
[2]*UK Astronomy Technology Centre, Royal Observatory, Blackford Hill, Edinburgh EH9 3HJ, UK*
[3]*Institute for Astronomy, University of Edinburgh, Royal Observatory, Blackford Hill, Edinburgh EH9 3HJ, UK*
[4]*Herzberg Institute of Astrophysics, National Research Council of Canada, Victoria, BC V9E2E7, Canada*
[5]*Department of Physics and Astronomy, University of Victoria, Victoria, BC V8W 3P6, Canada*
[6]*Observatoire de Paris, CNRS, 61 Av. de l'Observatoire, F-75014 Paris, France*
[7]*SRON Netherlands Institute for Space Research, PO Box 800, NL-9700 AV Groningen, the Netherlands*
[8]*School of Physics and Astronomy, University of St. Andrews, North Haugh, St. Andrews, Fife KY16 9SS, UK*
[9]*Departamento de Física Teórica, Universidad Autónoma de Madrid, Cantoblanco, E-28049 Madrid, Spain*
[10]*European Southern Observatory/Joint ALMA Office, Alonso de Cordova 3107, Santiago, Chile*
[11]*Astrophysics Group, Imperial College London, Blackett Laboratory, Prince Consort Road, London SW7 2AZ, UK*

Accepted 2013 July 15. Received 2013 July 15; in original form 2013 February 8

ABSTRACT

New detections of debris discs at submillimetre wavelengths present highly valuable complementary information to prior observations of these sources at shorter wavelengths. Characterization of discs through spectral energy distribution modelling including the submillimetre fluxes is essential for our basic understanding of disc mass and temperature, and presents a starting point for further studies using millimetre interferometric observations. In the framework of the ongoing SCUBA-2 Observations of Nearby Stars, the instrument SCUBA-2 on the James Clerk Maxwell Telescope was used to provide measurements of 450 and 850 μm fluxes towards a large sample of nearby main-sequence stars with debris discs detected previously at shorter wavelengths. We present the first results from the ongoing survey, concerning 850 μm detections and 450 μm upper limits towards 10 stars, the majority of which are detected at submillimetre wavelengths for the first time. One, or possibly two, of these new detections is likely a background source. We fit the spectral energy distributions of the star+disc systems with a blackbody emission approach and derive characteristic disc temperatures. We use these temperatures to convert the observed fluxes to disc masses. We obtain a range of disc masses from 0.001 to 0.1 $M_\oplus$, values similar to the prior dust mass measurements towards debris discs. There is no evidence for evolution in dust mass with age on the main sequence, and indeed the upper envelope remains relatively flat at $\approx$0.5 $M_\oplus$ at all ages. The inferred disc masses are lower than those from disc detections around pre-main-sequence stars, which may indicate a depletion of solid mass. This may also be due to a change in disc opacity, though limited sensitivity means that it is not yet known what fraction of pre-main-sequence stars have discs with dust masses similar to debris disc levels. New, high-sensitivity detections are a path towards investigating the trends in dust mass evolution.

Key words: techniques: imaging spectroscopy – circumstellar matter – submillimetre: planetary systems – submillimetre: stars.

1 INTRODUCTION

Discs of dynamically processed dust, rocks and asteroids surround at least 15 per cent of nearby Sun-like main-sequence stars (e.g. Trilling et al. 2008). Observations in the mid- and far-infrared (mid- and far-IR) with *Spitzer* and *Herschel* have shown that a fraction of cold discs may have been missed at shorter wavelengths. So far, submillimetre interferometers have allowed detailed imaging and characterization of the mass, radial distribution and temperature of millimetre dust grains in about a dozen of the brightest debris discs, but lacked sensitivity to study these objects in a systematic

⋆ E-mail: opanic@ast.cam.ac.uk

way. With the Atacama Large Millimeter/sub-millimeter Array (ALMA), a continuation of such detailed studies of debris discs will be possible, and the first identifications of possible targets with a single-dish submillimetre telescope like the James Clerk Maxwell Telescope (JCMT) present a stepping stone into this new era.

The SCUBA-2 Observations of Nearby Stars (SONS; Matthews et al. 2013), part of the JCMT Legacy Survey, aims to find excess submillimetre emission around nearby main-sequence stars known to be surrounded by debris discs, as witnessed by substantial excess emission above the stellar photosphere at one or more wavelengths, and in some cases, resolved images of the disc. It employs the SCUBA-2 submillimetre camera (Holland et al. 2013) on JCMT,[1] observing simultaneously at 850 μm as well as at 450 μm. With new detections of discs in the submillimetre, this instrument allows complementary studies to those carried out with *Herschel* at shorter wavelengths, and provides well-characterized targets for follow-up studies with ALMA at similar and longer wavelengths. Measurements of submillimetre thermal continuum emission are sensitive to the mass of dust contained in millimetre-sized grains, thus tracing emission from regions where disc material is replenished by collisions between larger objects. This is particularly important for those discs where the belts are sculpted by orbiting planets as millimetre dust is a reliable proxy for larger, gravity-dominated, bodies. It is necessary to study the millimetre data in combination with data from shorter wavelengths to best constrain the disc mass. Particularly useful is the modelling of the disc spectral energy distribution (SED), which, when encompassing a large range of wavelengths, yields the characteristic temperature, crucial for the interpretation. Ideally, SED modelling is combined with spatial information from imaging to remove some of the main parameter degeneracies.

In this paper, we present detections of submillimetre emission around main-sequence stars from the ongoing SONS survey. Section 2 summarizes the observations. In Section 3, we model the SED of our science targets, and take into account any available existing observations to best constrain the dust temperature, crucial for deriving a dust mass estimate from our observed submillimetre fluxes. We then constrain the basic disc parameters, including mass, and draw comparisons with a wider sample of discs detected so far in the millimetre. Our conclusions are summarized in Section 4.

2 OBSERVATIONS

Observational data presented in this paper were collected using the SCUBA-2 camera (Holland et al. 2013). Observations were taken as part of the SONS JCMT Legacy Survey over the period 2012 May to 2013 January. Individual observations were typically of 30 min, with total integration times per target varying from 1 to 4 hours with the overall goal of reaching an rms noise level of $<1.4\,\mathrm{mJy\,beam^{-1}}$ at 850 μm for each of the targets. The full width at half-maximum (FWHM) of the primary beam at 850 μm is 13 arcsec. Atmospheric opacity was monitored in real time using a line-of-sight water vapour monitor. During the observations the level of precipitable water vapour ranged from 1 to 2.4 mm corresponding to zenith sky opacities of $\tau_{850\,\mu\mathrm{m}} = 0.21$–$0.53$. The observations were taken with the constant speed DAISY pattern, which provides uniform exposure time coverage in the central 3-arcmin-diameter region of a field.

The data were reduced using the Dynamic Iterative Map-Maker within the STARLINK SMURF package (Chapin et al. 2013) using a configuration file specifically designed for faint, unresolved or compact sources. In this process, the data were frequency-domain, high-pass filtered at 1 Hz to remove residual low-frequency noise. This removes large-scale structures (either astronomical or instrumentally induced) greater than 150 arcsec, resulting in flat, uniform maps, largely devoid of gradients and artefacts. The data were flux calibrated against the primary calibrator Uranus and also secondary calibrators CRL 618 and CRL 2688 from the JCMT calibrator list (Dempsey et al. 2013). The estimated calibration uncertainties amount to 5 per cent at 850 μm and 10 per cent at 450 μm. The final images shown in the right-hand panels of Figs 1 and 2 have been smoothed with a 7 arcsec FWHM Gaussian to improve the signal-to-noise ratio (S/N). All targets discussed in this paper are spatially unresolved in our 13 arcsec resolution mapping, with $\leq 3\sigma$ emission outside the 13 arcsec diameter, centred on the peak of the emission. In the case of HD 161868, there is a marginal extension up to 4σ level in the E–W direction (Fig. 1, upper right-hand panel), but we do not consider this feature as significant (see Section 3.1.1). Observed peak fluxes and rms noise levels of these observations are given in Table 1.

The noise was estimated using multiple measurements of the flux densities, by integrating the flux within circular 13 arcsec beams placed 4 arcsec apart, over the central 3×3 arcmin^2 area. The resulting flux distributions were fitted by Gaussians with confidence level ≥ 97 per cent, and the noise levels reported in Table 1 correspond to the standard deviations of these fits. The number of beams with fluxes exceeding 3σ in the total sample of 10 3×3 arcmin^2 fields is consistent with the combined effect of the probability of a background source in the 3×3 arcmin^2 area (see Section 3.2) and the expectation for a normal distribution.

As can be seen in Figs 1 and 2, right-hand panels, some of the detections are offset as far as 5–7 arcsec from the locations of the target stars at the time of observations (the centre of the maps shown). Taking into account the pointing accuracy of JCMT (2 arcsec rms) and the astrometric uncertainty of the low-S/N detections, quadratically combined, it is possible that some of these detections do correspond to disc emission around the science targets. HD 17093, and possibly HD 205674, is more likely associated with a background object than a debris disc. In Section 3.1, we describe our modelling approach as well as results and implications for each star in our sample, while Section 3.2 discusses the probability of chance alignment with background sources.

3 RESULTS AND DISCUSSION

3.1 Modelling and derived dust masses

The observed SEDs have several data points in the regime where the excess emission is significantly greater than the star, therefore allowing an estimate of the temperature of the emitting dust. While the SEDs arise as the combined effect of dust grains of different sizes with different relative contributions to fluxes at different wavelengths, we use a simplified approach, in which the SEDs are modelled as dominated by a single-temperature component, seen as the temperature that is representative of the dust dominating the observed emission. In some cases, however, it is not possible to apply this approach. These are discs like HD 377, for example, where it is clear that the spectrum of the disc emission is broader than a single

[1] The JCMT is operated by the Joint Astronomy Centre on behalf of the Science and Technology Facilities Council of the UK, the Netherlands Organisation for Scientific Research and the National Research Council of Canada. Additional funds for the construction of SCUBA-2 were provided by the Canada Foundation for Innovation.

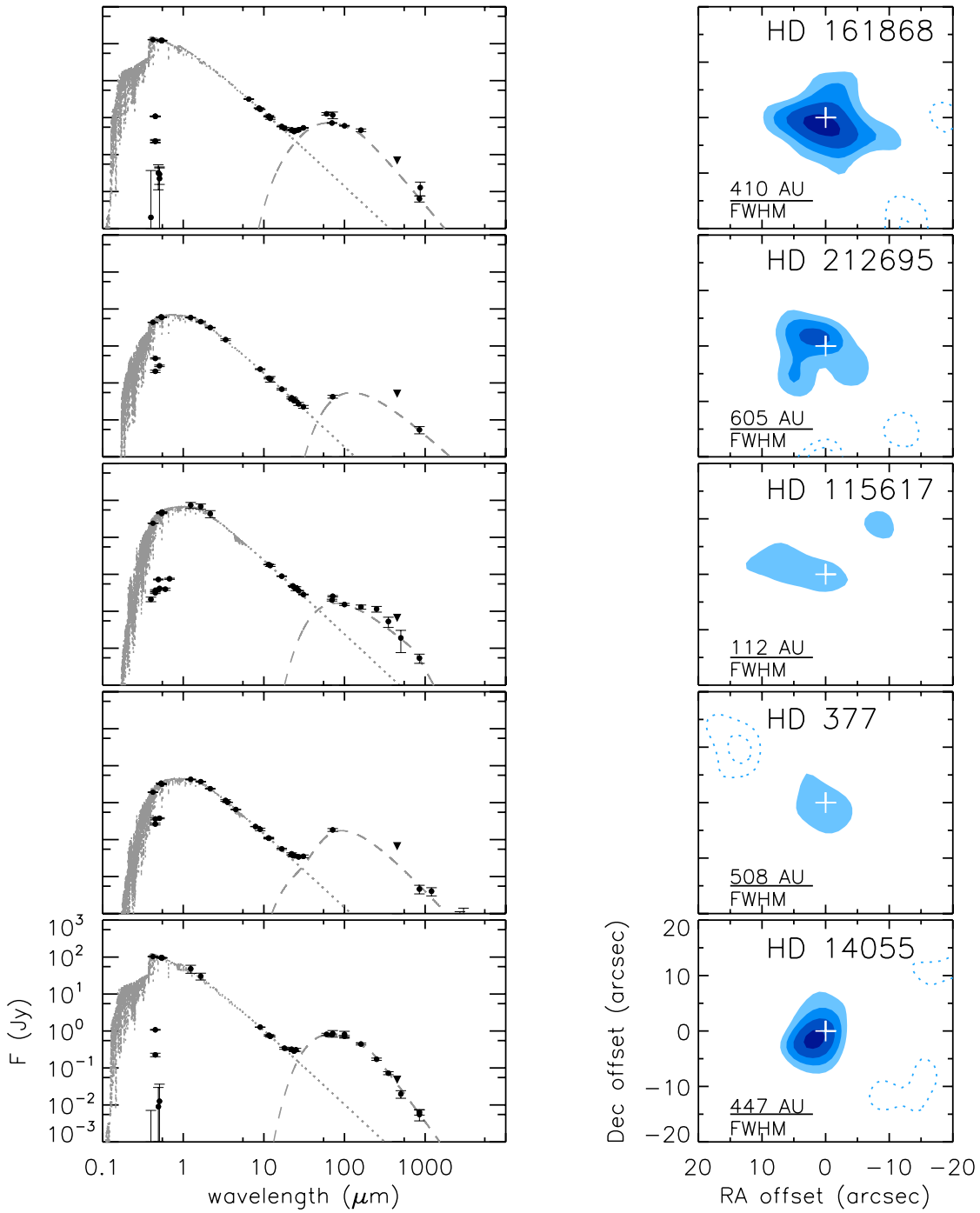

Figure 1. Left-hand panels: SEDs of our target stars (black filled circles), and the model fits to the stellar photospheric emission (dotted grey lines) and to the near-IR to millimetre excesses (dashed grey lines). The black triangles mark 450 μm upper limits. Right-hand panels: SCUBA-2 850 μm maps of the 40×40 arcsec^2 area centred on the stars (crosses). The spatial scales corresponding to the beam FWHM of 13 arcsec are indicated with bars. The contours are $1\sigma \times (\ldots -5, -4, -3, 3, 4, 5, \ldots)$ with the filled contours for positive and dashed contours for negative values. The 1σ levels can be found in Table 1. The figure continues in Fig. 2.

blackbody. In such cases, the disc is modelled with two-temperature components. Morales et al. (2011) interpret such two-temperature discs as corresponding to two spatially distinct concentric rings. However, such a spectrum could also arise from a single ring that has the appropriate grain properties and size distribution.

We model our targets following the approach described in Kennedy et al. (2012). The model is separated into two main components: a stellar atmosphere and a disc. Available short-wavelength (<10 μm) photometry from various sources including 2MASS, Tycho-2, *Hipparcos*, *Akari*, *IRAS* and *WISE* (Moshir et al. 1993; Hauck & Mermilliod 1997; Perryman & ESA 1997; Høg et al. 2000; Mermilliod 2006; Skrutskie et al. 2006; Ishihara et al. 2010; Wright et al. 2010) are used to fit stellar models by χ^2 minimization. This method uses synthetic photometry over known bandpasses. It has been verified against high-S/N 24 μm MIPS photometry for targets within the *Herschel* open time key project Disc Emission via a

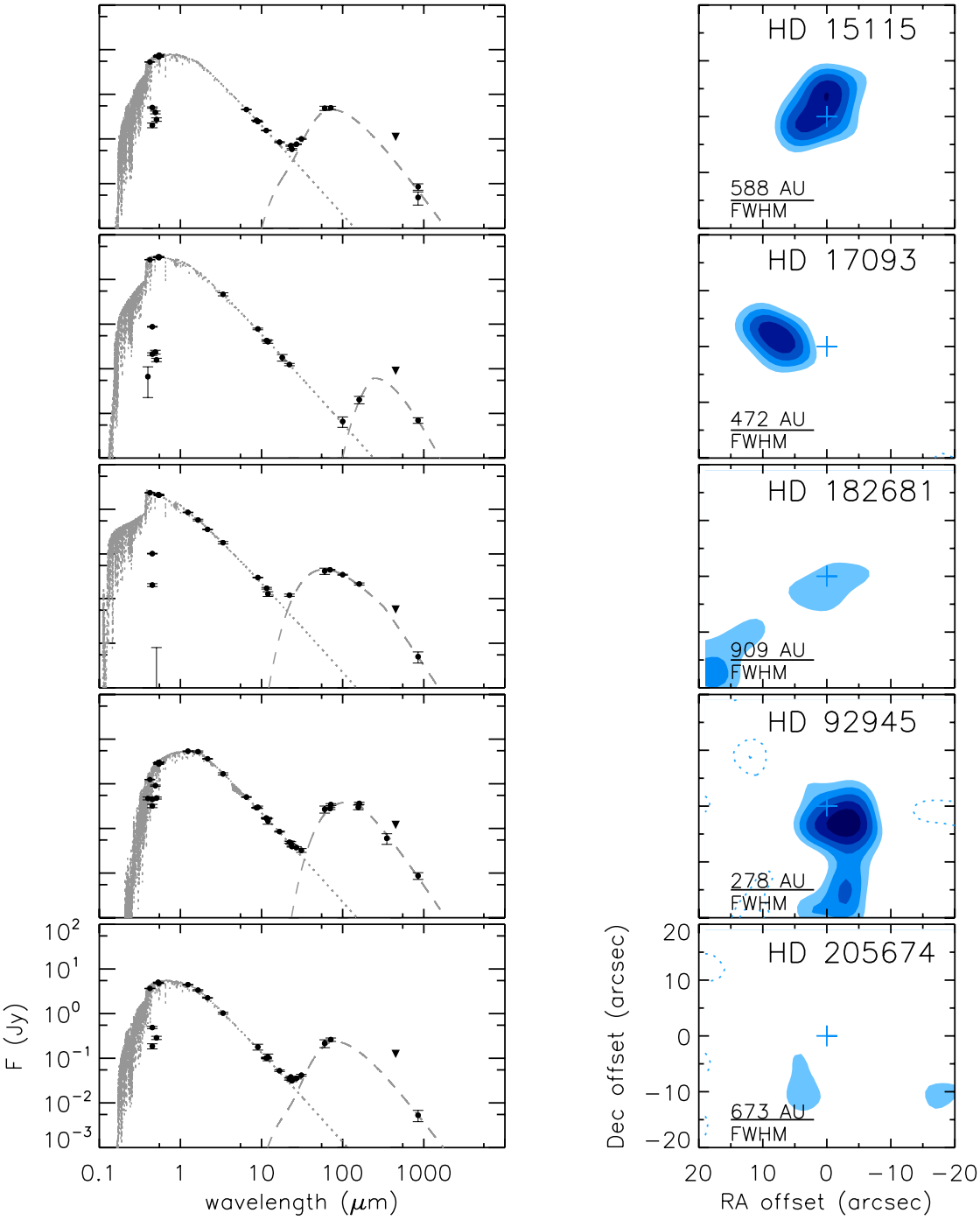

Figure 2. Fig. 1 continued.

Bias-free Reconnaissance in the Infared/Submillimetre (DEBRIS, Matthews et al., in preparation) and produces photospheric fluxes accurate to a few per cent for AFG-type stars.

The disc is modelled with one or two blackbody components, depending on the goodness of fit achieved by fitting a single blackbody to the observed excess emission. The model accounts for inefficient grain emission at long wavelengths by including parameters λ_0 and β, where the blackbody emission is multiplied by a factor $(\lambda/\lambda_0)^{-\beta}$ for wavelengths larger than λ_0. The best-fitting models are found by χ^2 minimization, where for single-temperature discs there are four parameters of temperature, normalization (the solid angle subtended by the dust, assuming blackbody behaviour), λ_0 and β. For two-temperature discs, we fix λ_0 and β to be the same for both components, so there are six parameters. Uncertainties are first estimated using the diagonal covariance matrix returned by the fitting routine. However, the parameters are commonly strongly correlated, so we use a full four-dimensional grid calculation around the best fit to obtain uncertainty estimates that are marginalized over the other parameters (using the standard $\Delta\chi^2$ method). For six-parameter models, we first subtract the warmer of the two disc components and then proceed with the four-dimensional calculation, because the warm emission does not affect the cool component and hence

Table 1. Summary of the science targets and SCUBA-2 450 and 850 μm observations. The first-time submillimetre detections are marked by asterisks. The distances are from the *Hipparcos* mission (van Leeuwen 2007). Two detections that are probably due to background galaxies (see text) are noted.

Object (HD)	Name	Spectral type	Distance (pc)	3σ upper limits at 450 μm (mJy)	Integrated flux at 850 μm (mJy)	Comment
161868	γ Oph	A0V	31.5	<69	6.4 ± 1.0	
212695*		F5	46.5	<51	5.4 ± 1.0	
115617*	61 Vir	G7V	8.6	<66	5.4 ± 1.4	
377*		G2V	39.1	<66	4.6 ± 1.2	
14055	γ Tri	A1V	34.4	<48	6.4 ± 1.1	
15115		F2	45.2	<111	8.5 ± 1.2	
17093*	38 Ari	A7III–IV	36.3	<90	7.0 ± 1.0	galaxy
182681*		B9V	69.9	<57	5.0 ± 1.3	
92945*		K1V	21.4	<120	8.7 ± 1.1	
205674*		F4IV	51.8	<125	5.3 ± 1.4	galaxy?

Table 2. Summary of the main derived parameters (with 1σ uncertainties or 3σ upper/lower limits). Fractional luminosities include both temperature components where they exist.

Object (HD)	Name	$L_{\rm disc}/L_\star$ (10^{-5})	$T_{\rm dust}$ (K)	$M_{\rm dust}$ ($0.01\,{\rm M}_\oplus$)	λ_0 (μm)	β
161868	γ Oph	9.9 ± 1	67 ± 4 and 147 ± 23	$2.7^{+0.2}_{-0.2}$	>60	>0.7
212695		7.9 ± 2	30^{+10}_{-7}	$12.8^{+9.7}_{-3.9}$	210[a]	1[a]
115617	61 Vir	2.8 ± 0.3	65 ± 3	$0.2^{+0.0}_{-0.0}$	–	–
377		37 ± 10	47 ± 11 and 131 ± 37	$4.4^{+1.7}_{-1.0}$	<750	–
14055	γ Tri	8.5 ± 0.4	76 ± 2	$2.7^{+0.1}_{-0.1}$	214 ± 17	1.1 ± 0.1
15115		53 ± 10	56 ± 9 and 146 ± 30	$8.9^{+0.2}_{-1.4}$	–	>0.3
17093[b]	38 Ari	0.17 ± 0.03	20	–	–	–
182681		25 ± 2	83 ± 2	$8.0^{+0.2}_{-0.2}$	–	>0.1
92945		62 ± 5	46^{+1}_{-3}	$2.6^{+0.2}_{-0.2}$	160^{+80}_{-30}	0.8 ± 0.2
205674[c]		36 ± 10	53 ± 4 and 151 ± 60	$7.8^{+0.8}_{-0.6}$	–	>0.1

[a]Based on Wyatt (2008). [b]Most likely a galaxy, see Section 3.1.7. A pure blackbody temperature is reported here. [c]Low S/N and large offset – possibly a galaxy.

the model constrains significantly (i.e. the warm components are relatively faint at far-IR and submillimetre wavelengths). Because the warm disc component is much fainter than the cool component at most wavelengths, only the Wien side of the warm component can be clearly separated from the cool component. Therefore, the bulk of the warm emission spectrum is poorly constrained, as are the derived warm-component fractional luminosities ($L_{\rm disc}/L_\star$), so we quote here the value for the entire disc. Assuming the same λ_0 and β as derived for the cool component, the warmer components typically have fractional luminosities that are 5–10 times fainter. The best-fitting models result in the parameters shown in Table 2.

Because our submillimetre observations are unresolved, they place only upper limits on the disc size and no information on disc structure. For targets that have been resolved with thermal or scattered light imaging, we take into account the results about the spatial structure when discussing our results, but do not impose those constraints on the SED modelling, as it is expected that the submillimetre emission traces preferentially larger dust than that traced at shorter wavelengths.

The observed 850 μm fluxes are used to derive the disc dust mass using the following relation:

$$M_{\rm dust} = \frac{F_\nu D^2}{\kappa B_\nu(T_{\rm dust})}, \quad (1)$$

where F_ν is the observed 850 μm flux, D is the distance of the star, κ is the dust opacity at 850 μm and $B_\nu(T_{\rm dust})$ is the Planck function at 850 μm for the dust temperature $T_{\rm dust}$. We adopt the dust temperature obtained from the SED modelling. From Fig. 2, it is clear that in the case of two temperatures, the colder component dominates the disc emission at the wavelength of our observations. For this reason, in our analysis of the 850 μm fluxes we adopt the lower of the two derived temperatures. To ensure consistency with prior works on submillimetre emission from debris discs, we adopt the commonly used value of $\kappa = 1.7$ cm^2 gm^{-1} (Zuckerman & Becklin 1993). The uncertainty ranges for the derived masses correspond to the maximum and minimum fluxes obtainable within the ranges of temperatures predicted by the SED fit.

3.1.1 HD 161868 (γ Oph)

The disc around this A0V type, 180^{+190}_{-170} Myr old, star (Song et al. 2001; Rieke et al. 2005) was imaged at 24 and 70 μm using *Spitzer* (Su et al. 2008). They measure the position angle (PA) and inclination of 50° and 55°, respectively. The derived inner and outer disc radius estimates of 13 and 520 au, respectively, make this disc one of the most extended debris discs. Our detection is marginally resolved, but a similar PA to that seen by *Spitzer* argues that the extension may be real. With an expected convolved size of about

20 arcsec for the 13 arcsec SCUBA-2 resolution, the marginal extension indicates that the millimetre grains are significantly less extended than the 10 times smaller particles probed in *Spitzer* observations. The first submillimetre measurements at 870 μm with the LABOCA bolometric array at the APEX telescope resulted in a marginal 2σ detection with an integrated flux of 12.8 ± 5.2 mJy (Nilsson et al. 2010). Our 6σ detection at 6.4 ± 1.0 mJy is roughly consistent with these prior observations. Our SED model reaffirms the results of Su et al. (2008), as we too find a need for a range of temperatures to reproduce the observed fluxes. The SED includes fluxes of 968 ± 50 mJy at 100 μm and 557 ± 30 mJy at 160 μm from *Herschel* observations (PI: Abraham). We use two temperatures of 147 and 67 K to fit the SED. The fit places constraints on $\lambda_0 > 60$ μm and $\beta > 0.7$. Assuming that most of the millimetre flux arises from the cold outer disc at 67 K, we derive a dust mass of $0.027\,M_\oplus$ in this debris disc.

3.1.2 HD 212695

Trilling et al. (2008) first detected excess emission associated with this star, at 70 μm. We report a 850 μm detection of 5.4 ± 1.0 mJy. For this F5 star, we fit the disc SED with a single temperature of 30 K. The blackbody emission in this model has $\lambda_0 = 210$ μm and $\beta = 1$, following Wyatt (2008). This is done because we do not have sufficient photometric information to fit a four-parameter model and constrain the modified blackbody parameters. Converted to dust mass, our submillimetre detection results in $0.128\,M_\oplus$, making this the most massive disc in our sample.

3.1.3 HD 115617 (61 Vir)

The nearby (8.55 pc), main-sequence G5 star 61 Vir hosts both a planetary system and a ring of planetesimals. Three low-mass planets (sub-Saturn mass) of minimum masses 5.3, 19 and $24\,M_\oplus$ at radial distances of 0.05, 0.22 and 0.48 au, respectively, have been detected around 61 Vir through radial velocity measurements (Vogt et al. 2010), with two of these confirmed in more recent HARPS observations (Wyatt et al. 2012). In the low-mass-planet systems, the incidence of detectable debris material appears to be greater than in systems with massive planets or with no planets at all according to the results of the survey of nearby G-stars hosting low-mass planets (Wyatt et al. 2012), taken within the *Herschel* open time key programme DEBRIS. The debris disc around 61 Vir has a fractional luminosity of 2×10^{-5} and was first identified with *Spitzer* observations (Bryden et al. 2006). *Herschel* imaging of the system at 70–500 μm reveals that the disc is located rather far from the planetary system, at distances of 30 au and greater. This disc is not expected to be influenced gravitationally by the detected planets, but the radial structure of the disc may hold important clues about how the disc has evolved and whether it is perturbed by any other unseen bodies at larger orbital distances.

The peak emission is detected in our SCUBA-2 image at 3.5σ eastwards from the star by about 7 arcsec, while the 3σ contour encircles the location of the star. As mentioned in Section 2, such an offset can be tolerated, considering the pointing accuracy and low S/N of our detection. There seems to be an elongation similar to the PA of 65° seen in *Herschel* images, where emission was resolved on scales of 15 arcsec (Wyatt et al. 2012). However, in the case of our 850 μm data, due to the low S/N we cannot draw conclusions about the structure of the emission. We fit the SED of this target with a single-temperature component at 65 K. Our 5.4 ± 1.4 mJy detection at 850 mJy yields a relatively low disc mass estimate of $0.002\,M_\oplus$.

Herschel images reveal two faint features distinct from the disc, at 27 arcsec W and 8 arcsec NNW of the star. Both features are brighter at longer wavelengths, and at 500 μm the NNW feature is inferred to be as bright as the disc. However, in our 850 μm data there is no detectable emission above 3σ noise levels (<4.2 mJy) at 27 arcsec W of the star. The latter source is just outside the 13 arcsec FWHM of our beam. There is a very localized 3σ signal to the NW of the star that potentially may arise from this feature (considering the offset tolerance).

3.1.4 HD 377

Our SED model for HD 377 results in two-temperature components, the hotter 131 K and the colder 47 K. A loose constraint is placed on the long-wavelength slope with λ_0 anywhere under 750 μm. Previous SED modelling (Morales et al. 2011) was also done using a warm and a cold component, and yielded temperatures of 183 and 52 K, respectively. Observed fluxes at 1.2, 2.7 and 3.0 mm for this debris disc are 4.0, 0.32 and 0.79 mJy, respectively (see Greaves et al. 2012, and references therein). From our submillimetre detection of 4.6 ± 1.2 mJy at 850 μm, we obtain a mass estimate of $0.044\,M_\oplus$ in dust. While we use a uniform approach, adopting the same dust opacity for all targets, Greaves et al. (2012) use a more informed dust opacity estimate in the regime more sensitive to larger grains, yielding a higher mass of $0.3\,M_\oplus$.

3.1.5 HD 14055 (γ Tri)

Our 6.4 ± 1.1 mJy detection agrees with the marginal 3σ 850 μm detection of this disc of 5.5 ± 1.8 mJy (Williams & Andrews 2006). Although it is notable that the spatially resolved PACS images could not be well fitted by a narrow ring, instead requiring the dust to be spread over a broad range of radii (Booth et al. 2013), our SED model of γ Tri consists of a single temperature of 76 K. This example stresses the complementarity of disc imaging at long wavelengths to the SED modelling, as broad cold components or multiple rings at large distances from the star are difficult to distinguish from a single component if SED analysis alone is used. Although it is not significantly resolved, our 850 μm image is slightly elongated in the direction of the measured 160° PA of this nearly-edge-on disc (Booth et al. 2013). Using our model, and the observed 850 μm flux, we derive a dust mass of $0.027\,M_\oplus$ for the disc around γ Tri.

3.1.6 HD 15115

An F2 star belonging to the β Pic moving group (12 Myr), the debris disc around HD 15115 has been previously imaged using the *Hubble Space Telescope* (*HST*) and Keck (Kalas, Fitzgerald & Graham 2007). These data show an evident asymmetry in the close-to-edge-on disc, seen as an elongated feature on the west side (PA = 78°) extending to 12 arcsec from the star, with only a weak counterpart on the east side. The morphology of the disc seen in scattered light is not expected to coincide with that in the millimetre regime, as very small dust particles are far more susceptible to radiation pressure than millimetre-sized grains. Again, the emission is not significantly spatially resolved. The peak emission in our SCUBA-2 observations is located about 5 arcsec away from the stellar position, but this effect is not relevant because the contour

at 6σ encircles the location of the star. In the submillimetre, the dust continuum emission from HD 15115 at 850 μm has first been detected by Williams & Andrews (2006), who derive the dust mass of 0.047 $M_\oplus$ by assuming a somewhat higher dust temperature of 62 K than our derived 56 K value. The discrepancy is primarily due to their 3σ detection of 4.9 ± 1.6 mJy being somewhat lower than our 8.5 ± 1.2 mJy SCUBA-2 detection. We derive a disc mass of 0.089 $M_\oplus$ from our submillimetre flux measurement. Our SED fit produces a constraint of $\beta > 0.3$.

3.1.7 HD 17093 (38 Ari)

The SCUBA-2 detection of HD 17093 is unlikely to be due to a debris disc for several reasons. The blackbody model results in a temperature of 20 K. If we assume that the emission is from dust grains that emit like blackbodies in thermal equilibrium, we obtain a stellocentric radius for the emission of 17.5 arcsec, at a distance of 36 pc. Emission from the small grains in debris discs typically exceeds the blackbody temperatures, so we would expect the disc emission to originate beyond this radius. The detection in our SCUBA-2 image (Fig. 2) is inconsistent with this expectation, because it is spatially unresolved and located within this 17.5 arcsec radius. Furthermore, there is a 7 arcsec offset of the SCUBA-2 emission E from the stellar position, which is approximately three times the SCUBA-2 1σ pointing accuracy. The offset of the star from the *Hipparcos*-expected position when it was observed by *WISE* in 2010 is only 0.2 arcsec, so there is no reason to believe that the *Hipparcos* position is significantly in error. Finally, the *Herschel*-PACS archive images of HD 17093 show significant 160 μm emission with the same offset as seen in the SCUBA-2 images (the origin of the 160 μm flux in Fig. 2). Therefore, we conclude that the 850 μm emission observed 7 arcsec east of HD 17093 is due to a background galaxy and is not associated with the star. Both the SCUBA-2 and the PACS 160 μm sources show the same offset. We therefore conclude that the PACS emission is also not associated with HD 17093 and that this star's debris disc has not yet been detected.

3.1.8 HD 182681

Excess emission around the relatively young (5 Myr), B9-type main-sequence star HD 182681 was first detected by Rhee et al. (2007), in 60 μm *IRAS* observations. We model the disc around HD 182681 with a single ring with a dust temperature of 83 K. Our SED fit produces a constraint of $\beta > 0.1$. The SED includes fluxes from spatially resolved *Herschel* data (PI: Abraham): 557 ± 30 Jy at 70 μm, 428 ± 20 Jy at 100 μm and 221 ± 12 Jy at 160 μm. *Herschel* images indicate a PA of about 45°. From our SCUBA-2 detection of 5.0 ± 1.3 mJy, we derive 0.08 $M_\oplus$. This is one of the higher masses derived in our sample.

3.1.9 HD 92945

We detect 850 μm emission near the location of the star, offset by 5 arcsec in the west of south-west direction, at 8.7 ± 1.1 mJy. As discussed in Section 2, such an offset is statistically consistent with the uncertainty combining pointing error and astrometric uncertainty. The disc around this K1 star has been imaged in scattered light with *HST* (Golimowski et al. 2011). Small dust in the disc is seen to extend 2–5.1 arcsec from the star (40–110 au). The near-IR brightness profile appears to have two distinct radial components, although these components are not distinguishable in the SED, which we fit with a single-temperature component of 46 K. The far-IR SED includes fluxes of 274 ± 15 mJy at 70 μm and 350 ± 20 mJy at 160 μm from *Herschel* observations (PI: Bryden). A realistic dust grain model was used in Golimowski et al. (2011) and one of the features of their model of HD 92945 is different dust sizes for the two components. They exclude the possibility that the grains emit as blackbodies, as their observed disc radii are inconsistent with such models. They derive the dust mass of 0.001 $M_\oplus$, but relying only on measurements shortwards of 350 μm. Such a mass estimate is difficult to compare to our submillimetre results, because theoretical extrapolation to longer wavelengths is unreliable. Our 850 μm flux predominantly traces larger, millimetre-sized particles, and we derive a dust mass of 0.026 $M_\oplus$ for the disc around HD 92945. Our SED model yields $\lambda_0 = 160^{+80}_{-30}$ μm and $\beta = 0.8 \pm 0.2$.

3.1.10 HD 205674

We detect 5.3 ± 1.4 mJy flux at 850 μm at a location offset by 10 arcsec from the star, in the SE direction. At low S/N it is difficult to establish whether the emission originates from the disc (see Section 2), and it may be a background source. Similarly to the cases of HD 161868, HD 377 and HD 15115, in the SED model we find it necessary to introduce a second temperature component to model the observed SED fluxes. Our two-temperature model consists of 151 and 53 K components. Using the latter, lower temperature, we derive a dust mass of 0.078 $M_\oplus$, at the high end of masses in our sample. Our SED fit produces a constraint of $\beta > 0.1$.

3.2 Confusion with background sources

At the observed flux levels, we can expect similar background sources to be present in our SCUBA-2 maps. At 850 μm these are predominantly high-redshift galaxies, and several (sub)millimetre surveys have derived expected densities of these sources for different areas on the sky. Except for HD 161868 (γ Oph), none of our science targets is aligned with star-forming regions, so we can exclude the probability of a chance alignment with young stellar objects, common millimetre sources in our Galaxy. There are no known young stellar objects in the surroundings of HD 161868 (γ Oph), our only star aligned with a star-forming cloud, nor any significant excess emission except at the location of the star itself (Fig. 1).

Following the estimate of 620 sources deg^{-2} above 5 mJy at 850 μm (Scott et al. 2002), we can expect 1.6 sources in each of our 3 arcmin maps, and 0.6 per cent probability of a background source at a flux level above 5 mJy within our 13 arcsec beam. So, for our stronger detections, i.e. those above 6 mJy level, it is safe to assume that the emission arises from our science targets and is not contamination due to background sources.

At lower flux levels, e.g. 3 mJy or approximately $2–3\sigma$ in our SCUBA-2 maps, we can expect five sources in each of our 3 arcmin maps (2000 sources deg^{-2} above 3 mJy at 850 μm, Eales et al. 2000). This corresponds to a probability of 2 per cent that a background source above 3 mJy is within the same beam as our detections. As discussed in Section3.1.7, HD 17093 is a very likely candidate for this scenario. For the vicinity of our targets in the sample shown here, i.e. the 10 40 $arcsec^2$ regions shown in the maps in Figs 1 and 2, we expect 2.4 sources above the 3 mJy level. This is consistent with some low-level emission seen at large offsets in the maps of HD 115617, HD 182681 and HD 205674.

Emission from the disc can be discerned from that of a background galaxy if the star is observed at a later epoch, following a significant change of location due to its proper motion. Of all our targets, only HD 115617 (61 Vir) exhibits a large proper motion of $(-1070.36, -1063.69)$ mas yr^{-1}, enabling such a test within a reasonable time-span, as shown in Wyatt et al. (2012). Another means of discrimination is spatially resolved imaging, through which the annular morphology of the emission would unequivocally indicate a disc origin. In the millimetre, such studies of debris discs will become more frequent with the high sensitivity provided by ALMA.

3.3 Dust mass evolution through the debris disc phase

Fig. 3 shows the measured dust masses of circumstellar discs during the pre- and main-sequence evolution of low-mass stars. The stellar masses of targets shown here span 0.2–3.3 $M_\odot$. All measurements are based on submillimetre and millimetre detections (850 μm–2.6 mm) of optically-thin thermal dust emission from a large compilation of literature data (see the caption of Fig. 3 for details). For uniformity, we adopt a constant dust opacity of 1.7 cm^2 g^{-1} (λ/850 μm) across all ages (Zuckerman & Becklin 1993). This is a standard value adopted in most submillimetre papers. To convert the flux to dust mass, we adopt average disc temperatures: 20 K for T Tauri stars, 50 K for Herbig Ae stars and for each main-sequence star we use a temperature corresponding to the blackbody fit to the disc emission, i.e. the same method as applied in Section 3.1. Optically thin to the stellar emission, the debris discs are heated more efficiently and are consequently warmer than protoplanetary discs. Using the above opacity and temperatures, we estimate the dust masses from the observed (sub-)millimetre fluxes of all sources shown in Fig. 3, using equation (1).

As can be seen in Fig. 3, the largest measured dust masses for debris discs from 10 to more than 1000 Myr are around $M_{\rm m.s.}(\max) = 0.5\,M_\oplus$, irrespective of age. The observable, small dust grains can originate from collisional evolution of dust and stochastic processes. Although dust is continuously lost from debris discs due to radiation pressure, the presence of massive and old discs suggests the existence of a sufficient reservoir of large particles to feed the range of dust sizes observable in the millimetre during 1000 Myr of exposure to direct stellar radiation. Observations of debris discs are severely affected by a detection bias because low-mass discs are only detectable around nearby, and therefore older, stars in the sample (Wyatt 2008). This effect can be seen in Fig. 3 where there are several targets at ages >500 Myr with derived masses lower than 0.01 $M_\oplus$ but none around younger stars, since such stars are more distant. This means that the decrease detected in the lower envelope of disc masses with age is due to an observational bias and not an indication of disc mass evolution. Surveys of debris discs in the (sub-)millimetre-wavelength regime are not yet complete enough to statistically compare the incidence of the observed massive ($\approx$0.5 $M_\oplus$) debris discs across ages from 10 to above 1000 Myr, and investigate possible evolutionary trends in mass distribution. Nonetheless, it is possible that disc mass remains nearly constant on the main sequence. The maximum mass of $\approx$0.5 $M_\oplus$

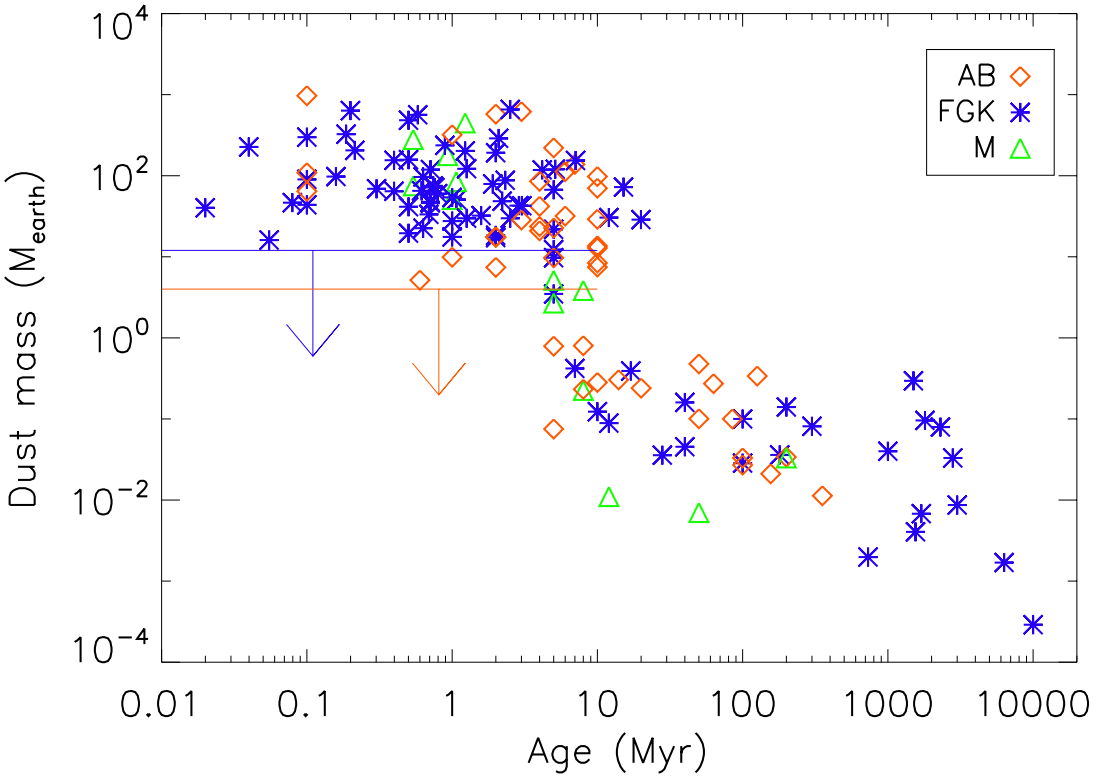

Figure 3. Dust masses of circumstellar discs derived based on observed (sub)millimetre fluxes towards pre-main-sequence and main-sequence stars. Observational limits corresponding to the sensitivity of a few mJy are shown with arrows: blue for 20 K discs around T Tauri stars and red for 50 K discs around Herbig Ae stars. Fluxes used in this plot are literature values from: Jewitt (1994), Osterloh & Beckwith (1995), Sylvester et al. (1996), Sylvester, Dunkin & Barlow (2001), Nuernberger, Chini & Zinnecker (1997), Nuernberger et al. (1998), Mannings & Sargent (1997, 2000), Holland et al. (1998, 2003), Greaves et al. (1998, 2004, 2005, 2012), Wyatt et al. (2005), Sheret, Dent & Wyatt (2004), Piétu, Dutrey & Kahane (2003), Piétu et al. (2006), Carpenter et al. (2005), Najita & Williams (2005), Williams & Andrews (2006), Lin et al. (2006), Matthews, Kalas & Wyatt (2007), Cieza et al. (2008), Roccatagliata et al. (2009), Ricci et al. (2010a,b), Nilsson et al. (2010), and the detections presented here.

measured here may be a few times larger if more realistic, lower dust emissivities are assumed for debris discs.

It is clear from Fig. 3 that a substantial fraction of discs around pre-main-sequence stars have dust masses larger than the highest derived masses for debris discs. It is not yet possible to determine at what age the massive young discs transition to the debris-like dust content – this may happen anywhere before 10–20 Myr, the age of oldest observed protoplanetary discs. Although the separation between the main-sequence and pre-main-sequence targets appears to be rather clear in Fig. 3, some debris discs are found to be as young as a few Myr, suggesting that there may be an unseen population of very young debris discs in the star-forming regions where massive discs are commonly found. A fraction of pre-main-sequence stars have no detectable IR excess, and it is very likely that discs around some of these stars have not completely dispersed but transitioned from an optically-thick to an optically-thin, debris-like, phase. Such debris discs are expected to exhibit an overall lower excess emission, and possibly a shallower long-wavelength slope, than in the case of gas-rich protoplanetary discs made of more pristine dust. Given the typical distance to the nearest star-forming regions of 140–300 pc, these youngest debris discs are faint and challenging to detect even if their mass was at the maximum debris disc mass seen on the main sequence of 0.5 $M_{\oplus}$.

To give a panoramic view of the current understanding of dust masses from the protoplanetary to debris disc phase, we used a uniform approach by assuming the same dust opacity for all targets in Fig. 3. However, it is expected that as the dust grows to cm sizes and beyond, the dust opacity decreases (e.g. Draine 2006). To constrain this property, and estimate dust masses more reliably, multiwavelength measurements in the millimetre regime and spatially resolved imaging are needed. Such work has been done for several samples of protoplanetary discs, yielding reliable dust mass estimates $\approx$0.01 $M_{\odot}$. However, direct imaging and detailed modelling of debris discs has been done for only a few brightest targets so far. Nevertheless, a general conclusion for debris discs is that, for their dust to be observable around stars that are $\gg$10 Myr, the observed dust must be fed by larger planetesimals (Backman & Paresce 1993), assuming that discs are steady-state phenomena (Wyatt et al. 2007). In the case of Fomalhaut, the conclusion was that the dust must be fed by >km-sized planetesimals in which case the true mass of solid material is at least two to three orders of magnitude larger than that inferred using the opacity assumed here. In other words, although Fig. 3 shows that the mass in millimetre- to centimetre-sized dust is significantly lower for main-sequence stars compared with the pre-main-sequence stars, this does not necessarily mean that the total solid masses are markedly different, as debris discs may contain a higher fraction of mass in larger bodies. The problem is that we cannot determine the mass contained in >kilometre-sized planetesimals observationally, in either debris or protoplanetary discs, and in particular for debris discs the majority of mass is expected to be contained in these large bodies.

To summarize, we cannot see evidence for a decrease in dust mass of debris discs with age on the main sequence, because there is currently no unbiased sample of (sub-)millimetre fluxes that can assess this. However, there appears to be a maximum dust mass of about 0.5 $M_{\oplus}$ in this stage (for the assumed dust opacity). The apparent sharp division in both age and mass between protoplanetary and debris discs is affected by the difficulties in detecting low-mass and debris discs around distant pre-main-sequence stars. It is also important to note that a sharp transition seen in Fig. 3 may be caused by an abrupt decrease in disc opacity as more mass is contained in larger, inefficiently emitting, bodies, rather than a scenario in which large amounts of mass are lost from the disc. With the ever-improving capabilities of ALMA, higher quality observational data over a range of submillimetre to millimetre wavelengths, we will begin to investigate the formation of debris discs and their dust mass evolution observationally.

4 CONCLUSIONS

We report 10 SONS detections at 850 μm with sensitivity of 1.0–1.4 mJy, obtained using the SCUBA-2 instrument. Of these, seven are first time 850 μm detections, and three are improvements in S/N over prior detections. While our observations are aimed at detecting dust around main-sequence stars, one, or possibly two, of the new detections is associated with a background object and not a debris disc. Within the 13 arcsec FWHM of the SCUBA-2 beam, corresponding to spatial scales of 100–900 au at the distances of our targets, none of our detections is significantly spatially resolved. We combine these detections with upper limits measured with SCUBA-2 at 450 μm, and *Herschel*-PACS photometry (where available), as well as any published fluxes from the literature. With modified blackbody emission models, we derive the characteristic temperature of the dust for each source. Several sources require two-temperature components, and/or long-wavelength modification of the blackbody emission to match all the observational constraints. With these models, and assuming a standard dust opacity, we convert the 850 μm fluxes to dust masses, in a range 0.001–0.1 $M_{\oplus}$. These values compare well with the previously derived values for debris discs and increase the total number of debris disc detections in the submillimetre. In comparison with the young population of discs around pre-main-sequence stars, the debris discs appear substantially less massive in dust. How and when the transition from the protoplanetary to the debris stage occurs, and how the debris disc mass evolves, is hard to establish due to instrument sensitivity coupled with diverse distances of stars with different ages. High-sensitivity ALMA observations leading to new detections of faint debris and protoplanetary discs is a promising prospect to address these fundamental questions.

ACKNOWLEDGEMENTS

The work of OP, MCW and GMK is supported by the European Union through ERC grant number 279973. The SCUBA-2 data were obtained under project MJLSD02. JPM is supported by Spanish grant AYA 2011-26202.

REFERENCES

Backman D. E., Paresce F., 1993, in Levy E. H., Lunine J. I., eds, Protostars and Planets III. Univ. Arizona Press, Tucson, p. 1253
Booth M. et al., 2013, MNRAS, 428, 1263
Bryden G. et al., 2006, ApJ, 636, 1098
Carpenter J. M., Wolf S., Schreyer K., Launhardt R., Henning T., 2005, AJ, 129, 1049
Chapin E. L., Berry D. S., Gibb A. G., Jenness T., Scott D., Tilanus R. P. J., Economou F., Holland W. S., 2013, MNRAS, 430, 2545
Cieza L. A., Swift J. J., Mathews G. S., Williams J. P., 2008, ApJ, 686, L115
Dempsey J. T. et al., 2013, MNRAS, 430, 2534
Draine B. T., 2006, ApJ, 636, 1114
Eales S., Lilly S., Webb T., Dunne L., Gear W., Clements D., Yun M., 2000, AJ, 120, 2244
Golimowski D. A. et al., 2011, AJ, 142, 30
Greaves J. S., Hales A. S., Mason B. S., Matthews B. C., 2012, MNRAS, 423, L70

Greaves J. S. et al., 1998, ApJ, 506, L133
Greaves J. S. et al., 2005, ApJ, 619, L187
Greaves J. S., Wyatt M. C., Holland W. S., Dent W. R. F., 2004, MNRAS, 351, L54
Hauck B., Mermilliod M., 1997, VizieR Online Data Catalog, 2215, 0
Høg E. et al., 2000, A&A, 355, L27
Holland W. S. et al., 2013, MNRAS, 430, 2513
Holland W. S. et al., 2003, ApJ, 582, 1141
Holland W. S. et al., 1998, Nat, 392, 788
Ishihara D. et al., 2010, A&A, 514, A1
Jewitt D. C., 1994, AJ, 108, 661
Kalas P., Fitzgerald M. P., Graham J. R., 2007, ApJ, 661, L85
Kennedy G. M., Wyatt M. C., Sibthorpe B., Phillips N. M., Matthews B. C., Greaves J. S., 2012, MNRAS, 426, 2115
Lin S.-Y., Ohashi N., Lim J., Ho P. T. P., Fukagawa M., Tamura M., 2006, ApJ, 645, 1297
Mannings V., Sargent A. I., 1997, ApJ, 490, 792
Mannings V., Sargent A. I., 2000, ApJ, 529, 391
Matthews B. C., Kalas P. G., Wyatt M. C., 2007, ApJ, 663, 1103
Matthews B. et al., 2013, JCMT Newslett., 34, 0
Mermilliod J. C., 2006, VizieR Online Data Catalog, 2168, 0
Morales F. Y., Rieke G. H., Werner M. W., Bryden G., Stapelfeldt K. R., Su K. Y. L., 2011, ApJ, 730, L29
Moshir M. et al., 1993, VizieR Online Data Catalog, 2156, 0
Najita J., Williams J. P., 2005, ApJ, 635, 625
Nilsson R. et al., 2010, A&A, 518, A40
Nuernberger D., Chini R., Zinnecker H., 1997, A&A, 324, 1036
Nuernberger D., Brandner W., Yorke H. W., Zinnecker H., 1998, A&A, 330, 549
Osterloh M., Beckwith S. V. W., 1995, ApJ, 439, 288
Perryman M. A. C. ESA, eds, 1997, The HIPPARCOS and TYCHO Catalogues. Astrometric and Photometric Star Catalogues Derived from the ESA HIPPARCOS Space Astrometry Mission. ESA, Noordwijk
Piétu V., Dutrey A., Kahane C., 2003, A&A, 398, 565
Piétu V., Dutrey A., Guilloteau S., Chapillon E., Pety J., 2006, A&A, 460, L43
Rhee J. H., Song I., Zuckerman B., McElwain M., 2007, ApJ, 660, 1556
Ricci L., Testi L., Natta A., Brooks K. J., 2010a, A&A, 521, A66
Ricci L., Testi L., Natta A., Neri R., Cabrit S., Herczeg G. J., 2010b, A&A, 512, A15
Rieke G. H. et al., 2005, ApJ, 620, 1010
Roccatagliata V., Henning T., Wolf S., Rodmann J., Corder S., Carpenter J. M., Meyer M. R., Dowell D., 2009, A&A, 497, 409
Scott S. E. et al., 2002, MNRAS, 331, 817
Sheret I., Dent W. R. F., Wyatt M. C., 2004, MNRAS, 348, 1282
Skrutskie M. F. et al., 2006, AJ, 131, 1163
Song I., Caillault J.-P., Barrado y Navascués D., Stauffer J. R., 2001, ApJ, 546, 352
Su K. Y. L., Rieke G. H., Stapelfeldt K. R., Smith P. S., Bryden G., Chen C. H., Trilling D. E., 2008, ApJ, 679, L125
Sylvester R. J., Skinner C. J., Barlow M. J., Mannings V., 1996, MNRAS, 279, 915
Sylvester R. J., Dunkin S. K., Barlow M. J., 2001, MNRAS, 327, 133
Trilling D. E. et al., 2008, ApJ, 674, 1086
van Leeuwen F., 2007, A&A, 474, 653
Vogt S. S. et al., 2010, ApJ, 708, 1366
Williams J. P., Andrews S. M., 2006, ApJ, 653, 1480
Wright E. L. et al., 2010, AJ, 140, 1868
Wyatt M. C., 2008, ARA&A, 46, 339
Wyatt M. C., Greaves J. S., Dent W. R. F., Coulson I. M., 2005, ApJ, 620, 492
Wyatt M. C., Smith R., Su K. Y. L., Rieke G. H., Greaves J. S., Beichman C. A., Bryden G., 2007, ApJ, 663, 365
Wyatt M. C. et al., 2012, MNRAS, 424, 1206
Zuckerman B., Becklin E. E., 1993, ApJ, 414, 793

This paper has been typeset from a TEX/LATEX file prepared by the author.